# Behaviors of heavy metal(loid)s in a cocontaminated alkaline paddy soil throughout the growth period of rice

Xiaofeng Zhang [a,b,c,1], Huanyun Yu [b,1], Fangbai Li [b,*], Liping Fang [b], Chuanping Liu [b], Weilin Huang [b], Yanhong Du [b], Yemian Peng [b], Qian Xu [b]

[a] Guangzhou Institute of Geochemistry, Chinese Academy of Sciences, Guangzhou 510640, PR China
[b] Guangdong Key Laboratory of Integrated Agro-environmental Pollution Control and Management, Guangdong Institute of Eco-environmental Science & Technology, Guangzhou 510650, PR China
[c] University of Chinese Academy of Sciences, Beijing 100049, PR China

## GRAPHICAL ABSTRACT
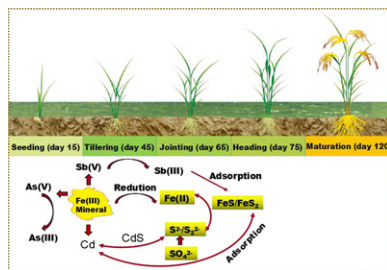


## ARTICLE INFO

## ABSTRACT

A pot experiment was conducted to investigate uptake of cadmium (Cd), arsenic (As) and antimony (Sb) by rice from a lime-treated paddy soil contaminated with the three pollutants. The results showed that the content of Cd in the total rice plants decreased as the plant grew, whereas the As and Sb contents increased steadily. The concentration of As in the pore water showed steady increase throughout the growth period, likely due to the reductive dissolution of iron (Fe)-bearing minerals and the reduction of As(V). In contrast, the concentrations of Cd and Sb in the pore water increased initially, likely attributable to the reductive dissolution of Fe-bearing minerals, and then decreased likely due to their adsorptions onto carbonate and Fe sulfides, the reduction of Sb(V), and the formation of CdS. A random forest model was used to quantitatively evaluate the relative contributions of environmental factors to the accumulation of Cd, As, and Sb in the rice plants. The results suggest that sulfides produced through sulfate reduction and the formation of Cd forms associated with sulfur (S) might significantly affected the Cd content in the rice plants. In addition, the dissolved Fe species, the oxidation–reduction potential, and the abundance of the As(V)-respiring gene were major contributors to the As content in the rice plants, suggesting the important role of the reduction of Fe-bearing minerals and As(V). The results also showed that the Sb content in the rice plants was correlated with Fe species, Sb(V) reduction, and acid volatile S. The environmental behaviors of Cd, As, and Sb in the cocontaminated paddy soil exhibited significant differences. Such differences should be considered in remedy of soils contaminated with multiple heavy metals and metalloids.

© 2019 Elsevier B.V. All rights reserved.

---

* Corresponding author.
  E-mail address: cefbli@soil.gd.cn (F. Li).
[1] These authors contributed equally to this work.

# 1. Introduction

Metallic and metalloid pollutants such as cadmium (Cd), arsenic (As), and antimony (Sb) are widespread in soils affected by mining activities during the process of mining and tailing disposal (Li et al., 2014; Okkenhaug et al., 2012; El Azhari et al., 2017). These pollutants enter various water bodies and eventually are accumulated in agricultural fields resulting from irrigation (Sheoran and Sheoran, 2006; Liu et al., 2013). Soil pollution leads to excessive heavy metals and metalloids accumulated in crops, which threatens human health (Järup, 2003; Zhuang et al., 2009). Heavy metals and metalloids accumulation in plants is particularly severe in southern China, where mining industry has been very active in the past four decades. Prior studies have reported high residual levels of Cd, As, and Sb in rice grains harvested from several mining areas of southern China that reach 2.76, 1.09, and 0.93 mg/kg, respectively (Williams et al., 2009; Liu et al., 2010; Wu et al., 2011).

The increased heavy metals and metalloids contents in rice grains in southern China has traditionally been interpreted via two major mechanisms. It is known that the acidic nature of red soils in South China favors the mobility of heavy metals and metalloids in soils. The soil acidity is thus mechanistically related to their increased uptake by rice plants. Moreover, irrigation using acid mine drainage (AMD) affected water for growing rice not only intensifies soil acidity but also adds loading of heavy metals and metalloids to the soil. Collectively, irrigation of polluted water ultimately promotes bioaccumulation of heavy metals and metalloids in plants. A common strategy for remedy of the soils polluted by heavy metals is to adjust the pH of polluted soils with alkaline materials such as lime, carbonates and phosphates. However, this strategy is not equally as effective as expected for all the heavy metals and metalloids. For example, lime treatments can effectively decrease the mobility and plant uptake of such cationic heavy metals as $Cd^{2+}$, $Pb^{2+}$ and $Zn^{2+}$ from soil (Lee et al., 2009), but cannot efficiently lower plant uptakes of anionic heavy metals(oids) such as As and Sb (Wilson et al., 2013).

Soils in mining areas are often polluted with multiple metals and metalloids such as Cd, As, and Sb. It is necessary to quantify the environmental behaviors of co-existing heavy metals and metalloids in such soils after treatment. However, mechanistic understanding of the behaviors of individual heavy metals and metalloids in cocontaminated soils is limited. The biogeochemical properties of heavy metals and metalloids vary greatly in soils. For example, Cd exists as a $Cd^{2+}$ cation in paddy soil. Increasing the pH or phosphate ligands of soil can promote the hydrolysis of $Cd^{2+}$ and form insoluble $Cd(OH)_2$ or $Cd_3(PO_4)_2$ owing to the strong coordination between $Cd^{2+}$ and electronegative $OH^-/PO_4^{3-}$ (Thawornchaisit and Polprasert, 2009). However, the chemical forms of As and Sb such as $AsO_3^{3-}/AsO_4^{3-}$ and $SbO_3^{3-}/SbO_4^{3-}$ are electronegative; thus, the higher negatively charged $OH^-/PO_4^{3-}$ in soil is not favorable for immobilizing As and Sb (Nakamaru and Altansuvd, 2014; Sigfusson et al., 2008; Cai et al., 2015). Unlike Cd, As and Sb have multiple valences and can undergo redox processes (Qi and Pichler, 2017). Even though As and Sb have similar redox potentials, they possess very different adsorption properties and immobilization when Fe-bearing minerals are present in soil (Dixit and Hering, 2003; Makris et al., 2009). In general, As(V) exhibits relatively stronger adsorption than As(III) whereas Sb(III) is more adsorptive than Sb(V) (Guo et al., 2014). Hence, the mobility and bioavailability of co-existing heavy metals and metalloids in soils may be very different when polluted soils are amended with lime for pH adjustment. Such variations are less studied previously and should be investigated.

It is known that AMD carries high levels of iron and sulfate, which can affect the behaviors of heavy metals and metalloids in soils (Hartley et al., 2004; Ke et al., 2014). Fe(III) can combine aqueous As/Sb to form stable precipitates (Guo et al., 2009; Wang et al., 2014), and its oxides and hydroxides have high adsorption capacities for Cd, As and Sb (Qi and Pichler, 2017; Lai et al., 2002) and also promote oxidation of As(III)/Sb(III) (Zhao et al., 2011; Qi and Pichler, 2016).

Meanwhile, $SO_4^{2-}$ can be reduced to $S_2^{2-}/S^{2-}$ in flooded soil, which could facilitate reactions with Cd, As, and Sb and form respective insoluble precipitates such as CdS, $As_2S_3$, and $Sb_2S_3$ under suitable redox and pH conditions (Zhang et al., 2008; Al-Sid-Cheikh et al., 2015; Herath et al., 2017). $S_2^{2-}/S^{2-}$ can also react with $Fe^{2+}$ to form Fe sulfides such as $FeS/FeS_2$ to adsorb Cd, As, and Sb (Karimian et al., 2018). In addition, soil microorganisms play an important role in the biological redox of heavy metals and metalloids such as As and Sb (Sun et al., 2016). For example, Mukhopadhyay et al. (2002) reported that As(V)-respiring bacteria play a key role in As(V) reduction.

This study was designed to test a hypothesis that individual metal or metalloid bound on soil reacts differently upon single treatments such as liming, hence the mobility and plant uptake differ among complex pollutants. Previous pot experiments focused mainly on the mobility and accumulation of heavy metals and metalloids at the maturation stage of rice (Ok et al., 2011; Zhu et al., 2010). However, the behaviors of heavy metals and metalloids in the soil–rice plant system may vary significantly during the entire growth period (Hashimoto and Yamaguchi, 2013; Zheng and Zhang, 2011). In this study, we collected samples of rice plants, pore water, and rhizosphere soils throughout the growth period of rice. The contents and chemical forms of Cd, As, Sb, and biogenic elements S and Fe in the samples were analyzed. In addition, the functional microbial gene abundance and diversity in the rhizosphere soil were characterized. The random forest (RF) model was used to estimate the importance of key environmental factors affecting the accumulations of heavy metal and metalloids in the rice. The objectives of this study were (i) to investigate the mobility and bioavailability of Cd, As, and Sb in a cocontaminated paddy soil after lime treatment; (ii) to identify the key environmental factors dominating the behaviors of Cd, As, and Sb in the cocontaminated paddy soil.

# 2. Materials and methods

## 2.1. Soil sampling and characterization

The paddy soil used in this study was collected in March 2017 at depths of 0–20 cm from a rice field contaminated with Cd, As, and Sb, which is located (111°27′ E, 27°42′ N) near the Xikuangshan mine of Hunan Province, China (Fig. S1). The soils were taken from three spots randomly located in a field. They were brought back to the lab, air-dried and passed through a 2-mm sieve, mixed to form a composite sample that was stored in jars before use for soil characterization and pot experiments. The composite soil was measured for its pH, contents of heavy metal and metalloids and key elemental compositions. The results showed that the soil was sandy loam with soil pH of 7.75 ± 0.15, soluble $SO_4^{2-}$ (Dis-$SO_4^{2-}$) content of 219 ± 25 mg/kg, total Fe (TFe) content of 34.2 ± 3.54 g/kg, Cd content of 3.65 ± 0.18 mg/kg, total As (TAs) content of 41.5 ± 3.57 mg/kg and total Sb (TSb) content of 185 ± 15.2 mg/kg. The contents of the other major elements in the contaminated soil were characterized using a wavelength dispersive X-ray fluorescence spectrometer (Magix PW-2403; PANalytical B.V., Almelo, Netherlands) as shown in Table S1. A comprehensive description of the characteristics of heavy metal and metalloid pollution in this mine has been provided by Li et al. (2017). High contents of Cd, As, and Sb in the soil were caused by occasional flooding and irrigation with AMD affected river water.

## 2.2. Pot experiment

The pot experiment was conducted in a climate-controlled greenhouse. Before planting, fertilizers containing 0.21 g urea, 0.455 g $K_2HPO_4 \cdot 3H_2O$, and 0.036 g $KH_2PO_4$ per kg of air-dried soil were applied to the soils and mixed thoroughly. The soils were immediately transferred into six identical 15-L pots, each containing 13 kg of the soil and submerged in water (2–3 cm above the soil surface) for 24 h. Huanghuazhan (Oryza sativa L. subsp. indica) seedlings of two-week

old were transplanted into each pot. Tap water was added daily for maintaining a water depth of 2–3 cm during the entire growth stage. After transplanting, soil pore water was collected from each pot on the days of 1, 3, 5, 7, 10, and 15 and then once every 10th day until day 115. The pore water sample was acidified with an appropriate amount of 1 M hydrochloric acid to keep the pH below 2.0 for preventing Fe precipitation and preserving As speciation (Zhao et al., 2013), and stored at 4 °C. Plant and soil samples were collected on days 15, 45, 65, 75, and 120, respectively, corresponding to the seedling, tillering, jointing, heading, and maturation stages. Meanwhile, soil samples were also collected from the pots on day 5. Each soil sample was split to two portions, a freezing-dried portion used for chemical analyses and a frozen one (−80 °C) used for DNA extraction. The plant samples were washed with deionized water, oven-dried at 65 °C, weighed for their dry biomass. The values of soil pH and oxidation–reduction potential (ORP) were also measured in situ using a portable digital pH/ORP analyzer (HQ11d; Hach, Loveland, Colorado, USA).

### 2.3. Analytical methods for pore water, soils, and rice plants

Concentrations of Fe, Cd, As, and Sb in pore water samples were analyzed after filtration through a 0.22 μm filter. The dissolved $Fe^{2+}$ (Dis-$Fe^{2+}$) and dissolved total Fe (Dis-TFe) were analyzed using the iMark microplate reader (Bio-Rad Laboratories, Hercules, California, USA). The concentration of dissolved Cd (Dis-Cd) was analyzed using graphite furnace atomic absorption spectrometer (PinAAcle 900; PerkinElmer, Boston, USA). Concentrations of dissolved As(III) (Dis-As(III)), dissolved total As (Dis-TAs), dissolved Sb(III) (Dis-Sb(III)) and dissolved total Sb (Dis-TSb) were analyzed using hydride generation atomic fluorescence spectrometry (HC-AFS) with an AS-30 instrument (Titan Instruments Co., Beijing, China).

Speciation of heavy metal and metalloids in soil were analyzed following the five-step sequential extraction procedure (SEP) described by Wenzel et al. (2001) and the European Community Bureau of Reference (BCR) sequential extraction procedure (Davidson et al., 1998) (Tables S2 and S3). In addition, 0.01 M $CaCl_2$ was used to extract exchangeable Cd (Salomon, 1998) (Table S2). The extraction and analysis methods of water-soluble sulfate and acid volatile sulfur (AVS) in soil, as described by Bak et al. (1991) and Simpson (2001), respectively, are shown in Table S4. The extraction and analytical methods of HCl-Fe (II) and amorphous iron oxide bound Fe (Oxalate-Fe) in soil are presented in the supporting information (Lovley and Elizabeth, 1988; McKeague and Day, 1966). The contents of heavy metal and metalloids in rice plants were analyzed following a standard procedure. In brief, 0.5 to 1.0 g dry weight of each plant sample was digested with 1.3 mL $HClO_4$ and 8.7 mL $HNO_3$ at 110–130 °C until a clear solution was obtained. The digested samples were filtered through a 0.45 μm filter and diluted to 50 mL with ultrapure deionized water. The Cd, As, and Sb concentrations were analyzed with the same methods described above.

### 2.4. Analytical methods for functional microorganisms in soil

The total DNA was extracted from the soil samples using a Power Soil Total DNA Isolation Kit (Mio Bio Laboratories, Inc., Carlsbad, California, USA) and following the manufacturer's instructions. The key functional genes including 16S ribosomal RNA (16S rRNA), arrA, the arsenate reductase gene (arsC), and the dissimilatory sulfite reductase beta-subunit gene (dsrB) were analyzed. Quantification of bacterial 16S rRNA, arrA, arsC, and dsrB genes was conducted using a CFX384 Touch real-time polymerase chain reaction (PCR) detection system (Bio-Rad Laboratories, Hercules, California, USA) and the SYBR® Green Supermix (Bio-Rad Laboratories). For each analysis, the 10 μL PCR reaction solution contained 5 μL of 2 × IQ SYBR® Green Supermix (Bio-Rad Laboratories), 0.1 μM of each primer, 6 mM of bovine serum albumin (BSA), and 0.5 μL of 0.5–5 ng DNA. The real-time PCR primers and conditions applied in each reaction are described in Table S5 (Einen et al.,

2008; Nadkarni et al., 2002; Sun et al., 2004; Mirza et al., 2017; Zheng et al., 2017); all quantitative PCR (qPCR) reactions of each sample were run in triplicate.

The microbial diversity in the arrA functional community was studied using high-throughput sequencing methods. First, the DNA was amplified based on PCR; the broad-range arrA primers are described in Table S5. Each PCR (50 μL reaction) contained 25 μL of 2 × Es Taq MasterMix (CW-Bio, Beijing, China), 0.5 μM of each primer, and 2.5 μL of DNA (<0.5 μg/50 μL). Then, replicate PCR products were pooled and purified using Agencourt AMPure PCR purification (Beckman Coulter, Georgia, USA) and the DNA concentration and quality were assessed using a Bioanalyzer 2100 (Agilent, Santa Clara, California, USA). Afterward, metagenomic libraries were constructed as described in the supporting information. Finally, the functional gene arrA was sequenced using the Illumina Genome Analyzer IIx test platform (San Diego, California, USA); the details are given in the supporting information.

### 2.5. Data reduction and statistics analysis

The accumulation amount (AA), contents of Cd, As, and Sb in total rice plants ($C_{total\ plant}$), bioconcentration factor (BCF), and transport factor (TF) were calculated using Eqs. (1)–(4) shown below.

$$AA : AA_{above\ part} = m_{above\ part} \times C_{above\ part}, AA_{root} = m_{root} \times C_{root}, AA_{total\ plant} = AA_{above\ part} + AA_{root}; \qquad (1)$$

$$C_{total\ plant} = \frac{m_{above\ part} \times C_{above\ part} + m_{root} \times C_{root}}{m_{above\ part} + m_{root}}; \qquad (2)$$

$$BCF : BCF_{total\ plant} = \frac{C_{total\ plant}}{C_{soil}}, BCF_{above\ part} = \frac{C_{above\ part}}{C_{soil}}, BCF_{root} = \frac{C_{root}}{C_{soil}}; \qquad (3)$$

$$TF = \frac{C_{above\ part}}{C_{root}}; \qquad (4)$$

where $AA_{total\ plant}$ (μg), $AA_{above\ part}$ (μg) and $AA_{root}$ (μg) are the accumulative amounts of Cd, As and Sb in total rice plants, plant part above the root and root, respectively; $C_{total\ plant}$ (mg/kg), $C_{above\ part}$ (mg/kg) and $C_{root}$ (mg/kg) are the content of total Cd, As, or Sb in total rice plants, plant part above the root and root, respectively; $m_{above\ part}$ (g) and $m_{root}$ (g) are the biomass of plant part above the root and root, respectively; $C_{soil}$ (mg/kg) is the content of total Cd, As, or Sb in the soil; Statistics analyses were performed for the heavy metal and metalloids data and abundance of key functional genes by using SPSS® 22.0 (IBM, Armonk, New York, USA). The statistical significance of the differences among treatments were determined via an analysis of variance with $p < 0.05$.

The sequencing data of the arrA gene were compared with those in the National Center for Biotechnology Information (NCBI) database to identify the microbial genera to determine the community composition. Moreover, to evaluate the factors affecting the contents of Cd, As, and Sb in rice, the RF model, an accurate learning algorithm, was used (Breiman, 2001a; Breiman, 2001b).

## 3. Results

### 3.1. Cd, As, and Sb accumulations in rice plants of different growth periods

The amounts of accumulated Cd, As, and Sb in the roots, parts above the roots, and the total rice plants are presented in Fig. 1. As a function of growing time, the amounts in each part of the rice plants all increased on the order of Cd > As > Sb before day 45 (tillering stage), and on the order of As > Cd > Sb after day 45. Moreover, after day 45 the accumulation amounts of Cd, As, and Sb in the total rice plants showed a sharp increase and eventually reached 70.5 ± 7.74, 696 ± 24.7, and 83.4 ± 12.7
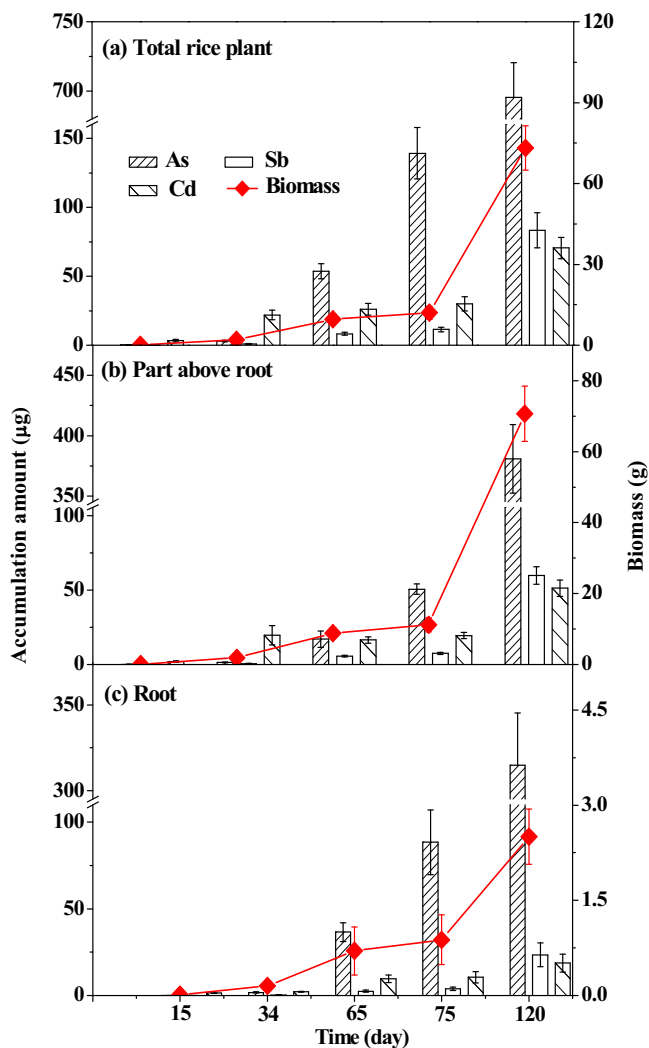
**Fig. 1.** Accumulation amounts of Cd, As and Sb and biomasses in total rice plants (a), parts above the roots (b) and roots (c) during the entire growth period. The data are the mean value ± SD (n = 3).

μg, respectively. The biomass of the plants showed a similar rapid increase from <2.0 g to >70 g after day 45. The accumulation amounts of Cd, As, and Sb in the roots and parts above the roots were similar; however, the average biomass of plant parts above the roots was an order of magnitude greater than that of the roots. This indicates a significant difference in the heavy metal and metalloid concentrations accumulated in the roots and parts above the roots.

As shown in Fig. S2(a), the contents of Cd, As, and Sb in the rice and the husk are very different, as As having the greatest contents whereas Sb having the lowest. The Cd content in the rice is $0.558 \pm 0.061$ mg/kg, which is much higher than the Cd limit of 0.20 mg/kg for rice set by the Chinese Standard (GB2762-2017). The As content in the rice is $1.39 \pm 0.14$ mg/kg, which is approximately twice as the allowable As limit of 0.50 mg/kg permitted by the Chinese Standard (GB2762-2017). The Sb content in the rice is $0.33 \pm 0.029$ mg/kg, which is also higher than the highest content of $0.19 \pm 0.01$ mg/kg reported previously by Wang et al. (2019). In the mature rice plants harvested on day 120, the average contents of Cd, As, and Sb in different rice tissues clearly decreased on the order of roots > parts above the roots > rice ≈ husk, with respective values of 7.07, 0.81, 0.56, and 0.53 mg/kg for Cd; 128, 8.05, 1.43, and 1.39 mg/kg for As, and 9.38, 1.14, 0.35, and 0.37 mg/kg for Sb. The calculated TF values of the rice plants were all significantly lower than 1, and the calculated root BCF values were always higher than those of the parts above the roots (Fig. S2(b) and Fig. 2). The BCF

value of Cd computed for the total rice plants varied from 0.26 to 5.27, which is higher than that (0.027–0.35) for As, and much higher than that (0.0024–0.0061) for Sb. These results indicate that the bioaccumulation ability of the rice plants followed the order of Cd > As > Sb (Fig. 2). Furthermore, the contents of Cd in the total rice plants decreased markedly from 19.2 mg/kg to <0.97 mg/kg as the plant grew over time, whereas those of As and Sb continued to increase from 1.12 to 14.5 mg/kg and from 0.45 to 1.15 mg/kg, respectively (Fig. 2).

### 3.2. Change trends of pH/ORP and Dis-Fe/Cd/As/Sb in pore water

Both the pH and ORP values of the soil pore water decreased initially and then maintained steady state values (Fig. 3(a) and (b)). At the final stage of growth, the pH maintained at approximately 7.2, and ORP value was approximately −250 mV. The Dis-TFe concentration increased steadily from below detection limit to 52 mg/L over time with the highest level in the last stage of growth (Fig. 3(c)). Similarly, steady increase was also detected for the Dis-TAs in pore water, which rose from a very low concentration to 30 μg/L (Fig. 3(e)). By contrast, the concentrations of the Dis-Cd and Dis-TSb displayed an initial rapid increase followed by much lower but sustained levels (Fig. 3(d) and (f)). The Dis-Cd concentration increased sharply from below the detection limit to a peak value of 2.9 μg/L on day 7 and subsequently decreased below 0.1 μg/L. Similarly, the Dis-TSb concentration initially increased sharply from lower than 300 μg/L to a peak value of 1204 μg/L on day 15, and then decreased abruptly to <8 μg/L.

Meanwhile, the contents of pore water As(III) and Sb(III) showed different trend of change over time. As(III) in the pore water increased steadily with time, but Sb(III) showed an initial increase and then abruptly decreased to minimal values. At their respective peak values, both As(III) and Sb(III) constituted as high as 94.5% and 85.0% of their respective total content in pore water (Fig. 3(e) and (f)). Overall, the concentrations of Cd, As, and Sb in the pore water followed the order of Sb > As > Cd, which is similar to the order of the three elements in the soil. It is interesting to notice that, among the three pollutants, only arsenic showed the synchronized trend of steady increase as a function of growth time in both pore water and rice plant. This indicates that accumulation of heavy metal and metalloid contents by rice plants may involve sophisticated mechanisms and processes and that pore water chemistry may not the only determining factor for uptake of Cd, As, and Sb by rice at its different stages of growth.

### 3.3. Changing trends of Cd, As, Sb, Fe, and S in rhizosphere soil

The exchangeable/adsorbed Cd, As, and Sb are considered as primarily bioavailable forms in soil (Ren et al., 2014; Wan et al., 2018) and are affected by changes in other extracted forms, as shown in Fig. 4. The $NH_3OH$-HCl-Cd and $CaCl_2$-Cd fractions decreased from 32.7% to 23.2% and from 0.41% to 0.13%, respectively, while the HAC-Cd and $H_2O_2$ + $NH_4AC$-Cd fractions increased from 21.6% to 35.5% and from 12.7% to 21.6%, respectively (Fig. 4(a)). These results indicate that Fe-Mn oxide-bound and exchangeable forms of Cd were transformed to carbonate- and organic-bound forms. Moreover, the decreasing trend of the exchangeable Cd fraction is consistent with that of Cd in the total rice plants. In contrast, the fractions of oxalate + ascorbic acid-As, oxalate-As, oxalate + ascorbic acid-Sb, and oxalate-Sb all decreased slightly (Fig. 4(b) and (c)). The $NH_4H_2PO_4$-Sb and $(NH_4)_2SO_4$-Sb fractions increased from 5.1% to 9.0% and from 5.6% to 9.6%, respectively. The $(NH_4)_2SO_4$-As fractions also showed an increasing trend, whereas the $NH_4H_2PO_4$-As fractions showed a fluctuating trend (Fig. 4(b)). The results may suggest that both well-crystallized and poorly crystallized hydrous oxide-bound Sb may gradually be transformed to non-specific/ specifically absorbed forms, whereas the As in the well-crystallized and poorly crystallized hydrous oxide-bound fractions may be primarily transformed into non-specific absorbed forms in the cocontaminated soil.
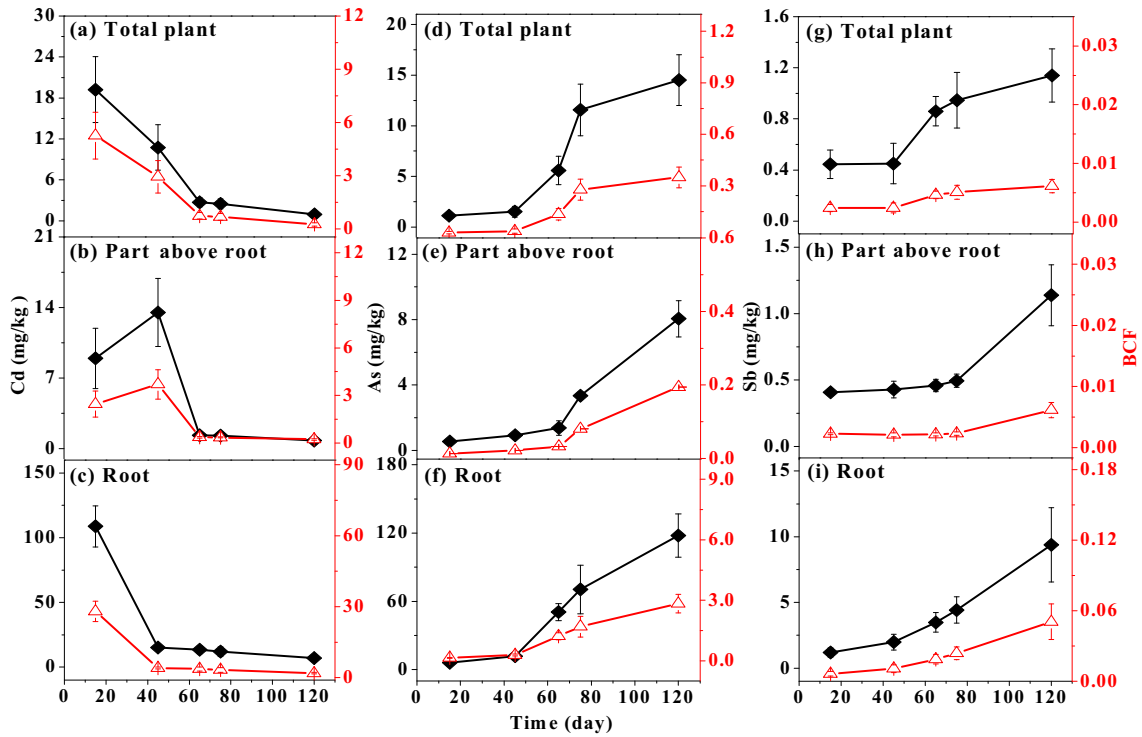
**Fig. 2.** Contents and BCF of Cd (a)/(b)/(c), As(d)/(e)/(f) and Sb(g)/(h)/(i) in different parts of rice plants during the entire growth period of the rice. The data are the means ± SD (n = 3).
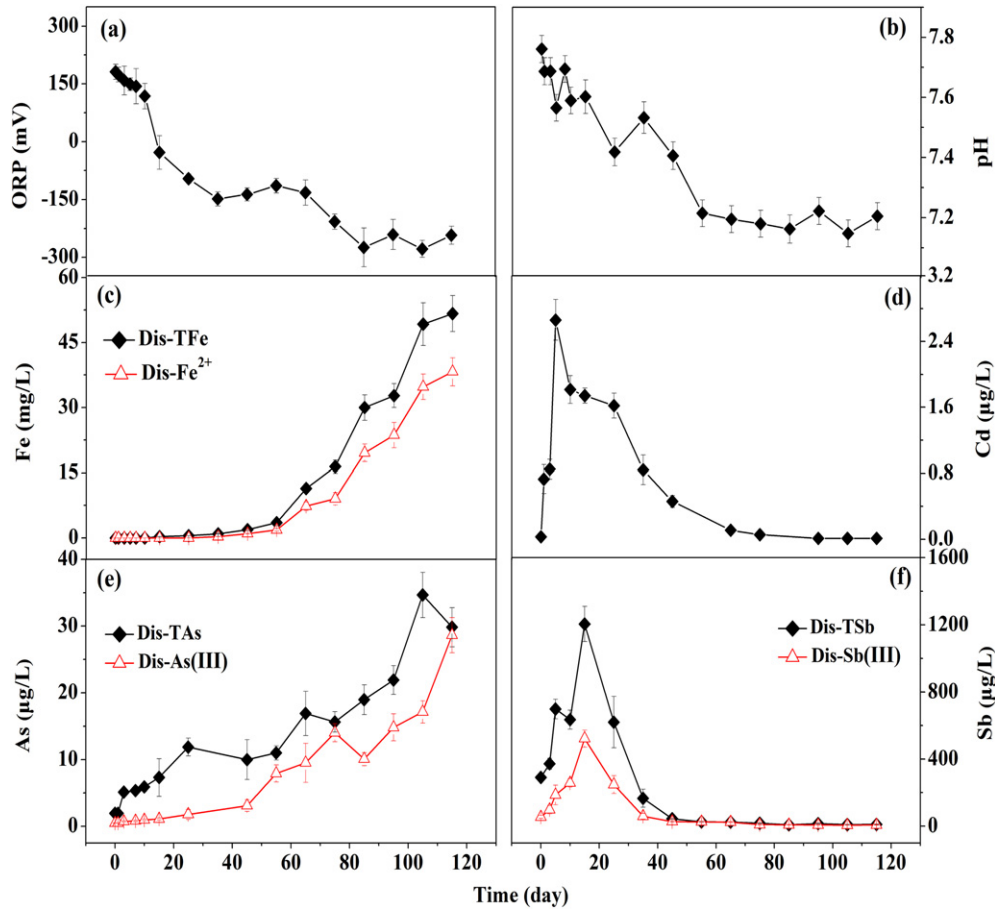


**Fig. 3.** ORP(a), pH(b) and concentrations of Dis-Cd(c)/As(d)/Sb(e)/Fe(f) in pore water during the entire growth period of the rice. The data are the means ± SD (n = 3).
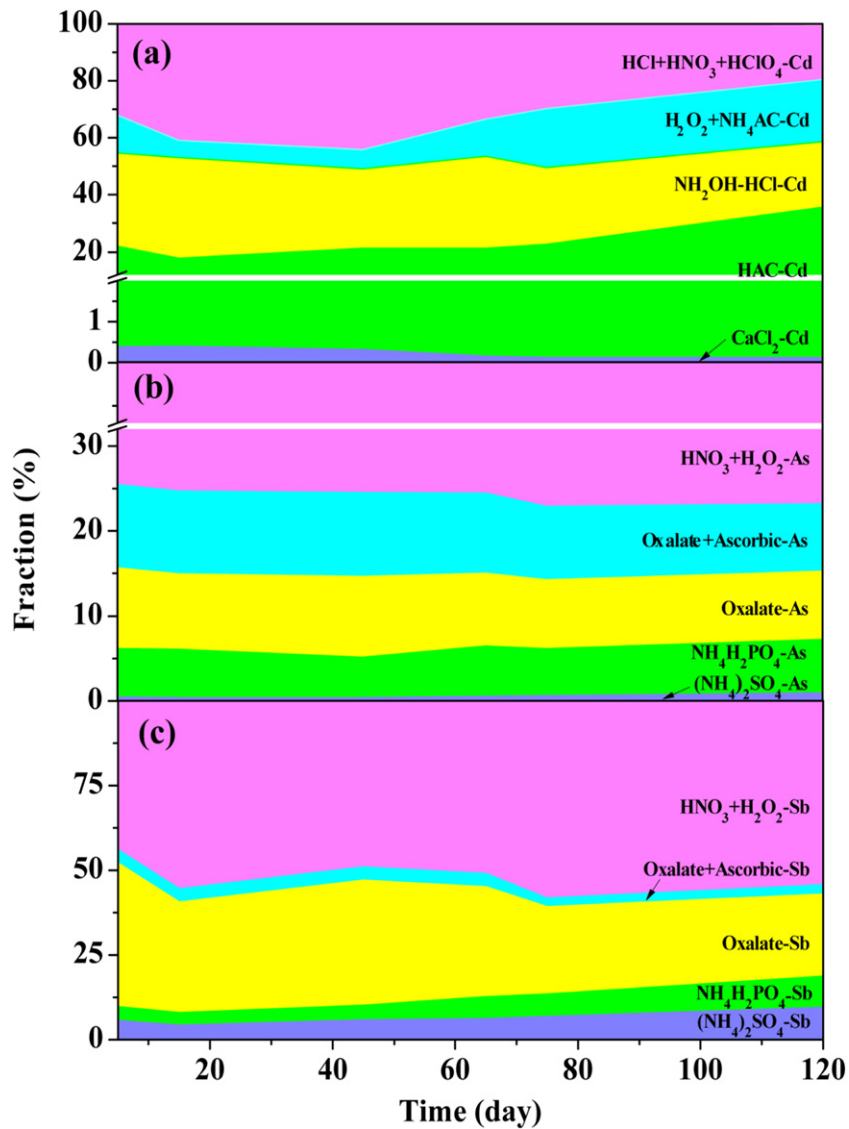
**Fig. 4.** Fractions of Cd(a), TAs(b) and TSb(c) in different extracted forms of rhizosphere soils during the entire growth period of the rice.

In general, the reduction of As(V)/Sb(V) can affect its mobility in soil (Weber et al., 2010; Li et al., 2018). The As(III) and Sb(III) contents extracted from the soil in different forms showed a slightly increasing trend; only $NH_4^+$-oxalate-Sb(III) (Fig. S3) mildly decreased, demonstrating that reduction in As(V)/Sb(V) is highly active in this flooded soil system. However, the proportions of extractable As (III)/Sb(III) in TAs/TSb were relatively low; the largest proportions of As(III) and Sb(III) were only 27.8% and 34.5% respectively, which are significantly lower than those in pore water. In addition, the As (III)/Sb(III) proportions in exchangeable and absorbed forms were still higher than those in the poorly crystallized hydrous oxide-bound form.
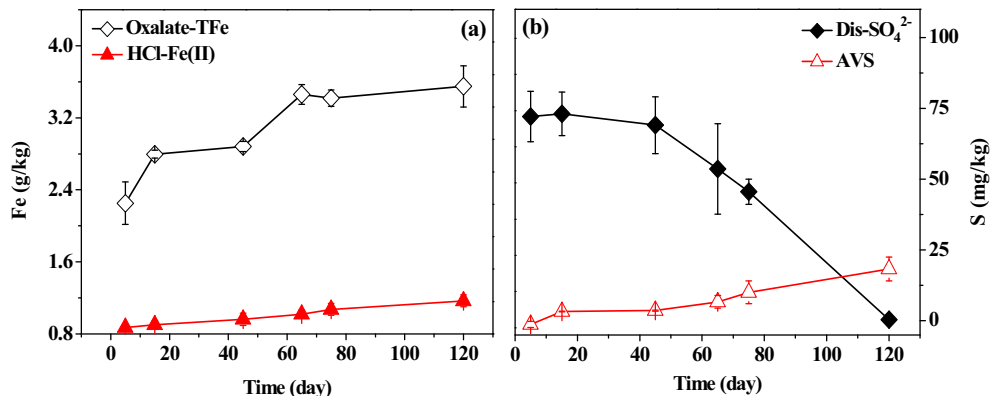


**Fig. 5.** Contents of Fe(a) and S(b) in different forms of cocontaminated soils during the entire growth period of the rice. The data are the means ± SD (n = 3).

Fig. 5 presents the contents of Fe and S in different chemical forms. The content of poorly crystallized Fe extracted by the $NH_4^+$-oxalate buffer increased significantly; this is consistent with a previous report stating that flooding conditions promote the transformation of crystalline Fe minerals in soils to poorly crystallized Fe (Li et al., 2004). The HCl-extractable Fe(II) also showed an increasing trend during the entire growth period of the rice, indicating the reduction dissolution of Fe minerals (Fu et al., 2016). The Dis-$SO_4^{2-}$ content in the soil declined markedly and the AVS content increased significantly from even <1.5 to approximately 20 mg/kg (Fig. 5(b)). This implies that the sulfate was gradually reduced to $S_2^{2-}/S^{2-}$ during the entire growth period of the rice.

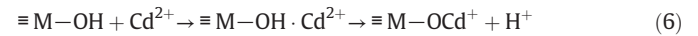### 3.4. Abundance and diversity of functional microorganisms in soil

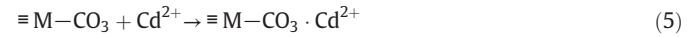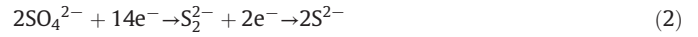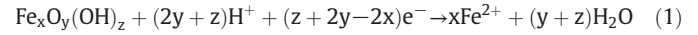The copy numbers of total bacteria showed an increasing trend ranging from $4.3 \times 10^7$ to $6.4 \times 10^7$ copies/g (Fig. S4(a)). Moreover, the abundance of the arrA gene, which contributes to extracellular As(V) reduction (Quéméneur et al., 2016), increased continuously from $3.0 \times 10^4$ to $8.7 \times 10^4$ copies/g. In addition, the abundance of the arsC gene, which contributes to intracellular As(V) reduction (Jackson and Dugas, 2003), showed a decreasing trend and was always significantly lower than that of the arrA gene (Fig. S4(b) and (c)). More importantly, the increasing trend of the arrA gene abundance was consistent with that of the As(III) content in the pore water (Figs. 3(e) and S4(b)), whereas the change trends of the arsC gene abundance and the As(III) content were quite different. This indicates that the reduction of As(V) was likely achieved by dissimilatory As(V)-respiring bacteria. Similar to that of As, the increasing trends of the Sb(III) concentrations in the pore water prior to day 15 (Fig. 3(f)) and in the non-specific/specifically absorbed forms (Fig. S3(d) and (e)) were also consistent with that of the arrA gene abundance. In addition, the abundance of the dsrB gene increased by four-fold, from $4.0 \times 10^5$ to $2.0 \times 10^6$ copies/g, which is consistent with the increasing trend of AVS in the soil (Fig. 5(b)). The diversity of the As(V)-respiring bacteria was also analyzed by high-throughput sequencing for the arrA gene (Fig. S5). *Geobacter* and *Desulfuromonas* were found to be the major As(V)-respiring genera of bacteria with abundances varying from 95.6% to 89.3% and 0.9% to 9.0%, respectively (Fig. S5).

## 4. Discussion

### 4.1. Cd migration, transformation, and affecting environmental factors

In flooded paddy soil, microbes can use root exudates as their carbon sources for growth and Fe(III)-bearing minerals as electron acceptors (Reaction (1)) (Favre et al., 2002; Kulkarni et al., 2018), yielding release of heavy metals (Fang et al., 2016; Hartley et al., 2004). It is consistent with our observations that the concentrations of Fe and Cd in the pore water increase prior to day 7 (Fig. 3). However, the Dis-$Cd^{2+}$ could be adsorbed onto carbonates and hydroxides (Reactions (5) and (6)) at pH > 7.25, but its concentration was not high enough to form $Cd(OH)_2$ (Fig. S6(a); Chuan et al., 1996). Thus, an obvious increase was found in the content of carbonate-bound Cd in the extracted soil (Fig. 4(a)). A previous study of Cd speciation in alkaline paddy soil also found that Cd carbonates are the major species during flooding periods and this fraction is less labile under alkaline conditions (Khaokaew et al., 2011). Moreover, in anaerobic and flooded paddy soil, $SO_4^{2-}$ can be used as an electron acceptor and be reduced to $S^{2-}/S_2^{2-}$ (Reaction (2)) (Fulda et al., 2013; Pallud and Van Cappellen, 2006) by sulfate reducing bacteria. Subsequently, $S_2^{2-}/S^{2-}$ can also react with $Fe^{2+}$ to form stable Fe sulfides ($FeS_2/FeS$) (Reactions (3) and (4)) (Fortin and Beveridge, 1997), which decreases the $SO_4^{2-}$ content and increases the content of AVS in the soil (Fig. 5(b)). In addition, some dissolved $Cd^{2+}$ can react with $S^{2-}$ to form CdS precipitation (Fig. S6(a)) or can be adsorbed directly by Fe sulfides (Reactions (7), (8) and (9)), which could increase

the organic form of Cd (Fig. 4(a)). The Cd concentrations in the pore water showed a rising trend and then decreased because they were affected by three chemical processes involving Cd, i.e., release, adsorption, and precipitation.

$$Fe_xO_y(OH)_z + (2y+z)H^+ + (z+2y-2x)e^- \rightarrow xFe^{2+} + (y+z)H_2O \quad (1)$$

$$2SO_4^{2-} + 14e^- \rightarrow S_2^{2-} + 2e^- \rightarrow 2S^{2-} \quad (2)$$

$$Fe^{2+} + S_2^{2-} \rightarrow FeS \quad (3)$$

$$Fe^{2+} + S^{2-} \rightarrow FeS \quad (4)$$

$$\equiv M-CO_3 + Cd^{2+} \rightarrow \equiv M-CO_3 \cdot Cd^{2+} \quad (5)$$

$$\equiv M-OH + Cd^{2+} \rightarrow \equiv M-OH \cdot Cd^{2+} \rightarrow \equiv M-OCd^+ + H^+ \quad (6)$$

$$Cd^{2+} + S^{2-} \rightarrow CdS \quad (7)$$

$$\equiv FeS_2 + Cd^{2+} \leftrightarrow \equiv FeS_2 \cdot Cd^{2+} \quad (8)$$

$$\equiv FeS + Cd^{2+} \leftrightarrow \equiv FeS \cdot Cd^{2+} \leftrightarrow \equiv CdS + Fe^{2+} \quad (9)$$

The RF model was adopted to further quantitatively evaluate the relative contributions of environmental factors to the Cd contents in the total rice plants. The variable importance and partial dependence of the responses of environmental factors including $SO_4^{2-}$, Dis-Cd, $CaCl_2$-Cd, HAC-Cd, $H_2O_2$-Cd, ORP, and AVS to changes in the Cd content in the total rice plants is shown in Fig. 6(a). The results from the RF model show that $CaCl_2$-Cd, Dis-Cd, AVS, ORP, $H_2O_2$-Cd, and $SO_4^{2-}$ were the greatest contributors to the Cd content in rice plants, with importance scores of 21.8%, 20.5%, 17.5%, 13.3%, 12.8%, and 9.8%, respectively (Fig. 6(a)). These results indicate that the process related to sulfur transformation, such as sulfate reduction and the reactions between sulfides and dissolved $Cd^{2+}$ or $Fe^{2+}$, significantly affect the Cd content in rice plants. This result differs from a previous study (Yu et al., 2016) that reported that pH and Fe species were the most important factors affecting Cd bioavailability. The difference should be attributable to the pH difference in the soils investigated. In the present study, although the pH showed a decreasing trend throughout the rice growth period (Fig. 3 (b)) likely due to $CO_2$ produced by organic matter decomposition, root exudation, and plant respiration (Reth et al., 2005; Hinsinger et al., 2003), the lowest pH was still higher than 7.2. In contrast, most of the soil (>90%) in the sampling region of the study by Yu et al. (2016) was acidic, and Cd existed mainly in the residual and Fe-Mn oxide-bound fractions. In the flooded alkaline paddy soil of the present study, carbonate-bound and sulfur-associated forms were the major fraction of Cd, which may decrease the Cd availability. Accordingly, the Cd content in the rice plants showed a deceasing trend during the entire rice growth period (Fig. 2).

### 4.2. As migration, transformation, and affecting environmental factors

As the measured ORP value decreases, the reductive dissolution of Fe-bearing minerals in soils occurs and As(V) and As(III) are released to the pore water or exposed on the surfaces of soil minerals (Pedersen et al., 2006). Accordingly, the As in well/poorly crystallized Fe-Al hydrous oxide-bound fractions decreased (Fig. 4(b)), and the dissolved and HCl-extracted Fe(II) increased (Figs. 3(c) and 5(a)). In the flooded paddy soil, the concentration of As(III) in pore water and the abundance of the arrA gene showed a simultaneous increase trend (Figs. 3(e) and S4(b)), suggesting that the As(V) reduction by As(V)-respiring bacteria, especially *Geobacter* and *Desulfuromonas*, could be promoted (Reaction (10)). Previous studies (Islam et al., 2004; Lear et al., 2007) also found that *Geobacter* species were abundant As(V)-respiring
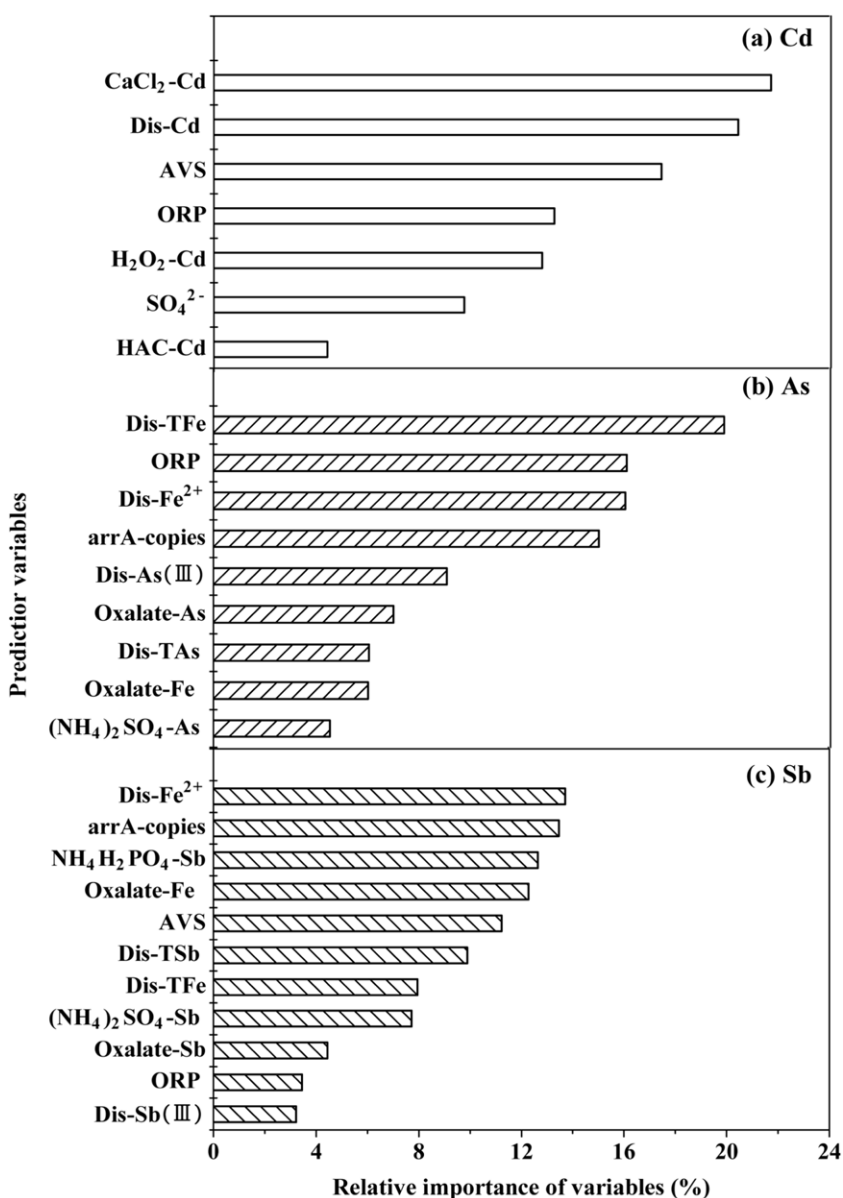
**Fig. 6.** Variable importance scores of the individual predictors for estimating the Cd(a), As(b) and Sb(c) accumulation in total rice plants based on random forest (RF). The importance scores of the independent variables were rescaled by setting their sum to 100%.

bacteria in arsenic-rich sediments and flooded paddy soil. *Geobacter* species are capable of reducing Fe(III) and identified as active iron-reducing bacteria in rice paddy soils (Hori et al., 2010). Similarly, members of the genus *Desulfuromonas* have an ability to respire both As(V) and Fe(III) and thus *Desulfuromonas* species may also play an important role in the mobilization of As and Fe (Osborne et al., 2015). Generally, As(III) is more mobile than As(V) in soil, and the enhanced reduction of As(V) can further promote the mobility of As (Kocar et al., 2006). Moreover, under high pH conditions, the dissolved As(III) in pore water do not easily to precipitate with $S^{2-}$ (Fig. S6(b); Couture and Van Cappellen, 2011); therefore, the concentrations of Dis-TAs and absorbed As fractions in soil, which are considered to be the most bioavailable portions in soil, increased (Figs. 3(e) and 4(b)) and further promoted As accumulation in the rice plant (Fig. 2).

The relative contribution of environmental factors to the As content in the total rice plants was evaluated quantitatively by using the RF model. The variable importance and partial dependence of the responses of environmental factors, such as ORP, Oxalate-Fe, Dis-$Fe^{2+}$/TFe, arrA gene copies, Dis-As(III), Dis-TAs, $(NH_4)_2SO_4$-As, $NH_4H_2PO_4$-
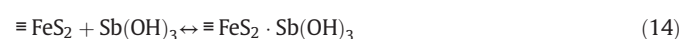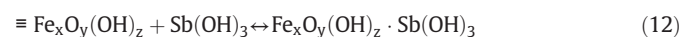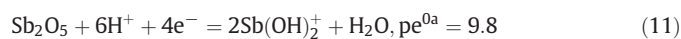
As, and Oxalate-As, to the As content in the total rice plants are indicated in Fig. 6(b), and the pseudo-$R^2$ value increased to 86.03% in the RF models. The main contributors to the As contents in the total rice plants were Dis-TFe, ORP, Dis-$Fe^{2+}$, arrA-copies, Dis-As(III), Oxalate-As, Dis-TAs, and Oxalate-Fe with corresponding importance scores of 19.9%, 16.1%, 16.0%, 15.0%, 9.1%, 7.0%, 6.1% and 6.0%, respectively. These results indicate that the dissolved Fe species, ORP, and the abundance of arrA determined the As content in the rice plant. Accordingly, the As content in the rice plants was primarily regulated by the reductive dissolution of Fe minerals and the reduction of As(V); similar results were obtained in previous research (Weber et al., 2010).

$$H_3AsO_4 + 2H^+ + 2e^- = H_3AsO_3 + H_2O, \, pe^{0a} = 9.5 \qquad (10)$$

### 4.3. Sb migration, transformation, and affecting environmental factors

The Sb content in the rice plants also increased during the entire lifecycle of the rice (Fig. 2(g), (h), and (i)) and the increase was

consistent with the variations of $(NH_4)_2SO_4$-Sb and $NH_4H_2PO_4$-Sb fractions in the soil (Fig. 4(c)). Similar to that of As, a decrease in ORP in anaerobic paddy soils likely resulted in the reductive dissolution of Fe-bearing minerals in the soil and the subsequent release of Sb(V) and Sb(III) into the pore water. Accordingly, the Sb in well-crystallized and poorly crystallized Fe-Al hydrous oxide-bound fractions decreased (Fig. 4(c)), and the dissolved Sb in the pore water increased prior to day 15 (Fig. 3(f)). Moreover, Sb(V) was likely reduced to Sb(III) by microorganisms (Reaction (11)). Both As and Sb have similar redox potentials (Reactions (10) and (11)) (Wilson et al., 2010). A previous study showed that, when both Sb and As are present, As(V) can compete with Sb(V) for electrons during anaerobic microbiological respiration (Kulp et al., 2013). Shotgun metagenomics analysis showed that microorganisms may use similar metabolic pathways to transform both As and Sb (Sun et al., 2017), and *Anaeromyxobacter* spp. are considered to have the potential for reducing both As(V) and Sb(V) (Xiao et al., 2016). In our study, the increasing trends of Sb(III) in the pore water prior to day 15 and the Sb(III) in the adsorbed fraction are consistent with that of arrA gene abundance. Thus, it is possible that the As(V) reducing microorganisms could also reduce Sb(V) in this soil. The resulting Sb(III) can be much more easily bound on soil minerals than Sb(V), yielding lowered concentration of Sb in pore water (Reaction (12) (Kong et al., 2015) or accumulation in other soil components (Ilgen and Trainor, 2011). Therefore, with a decrease of the Sb in well-crystallized and poorly crystallized oxide-bound fractions, the specifically and non-specifically absorbed Sb increased, and the dissolved Sb decreased after day 15 (Figs. 3(f) and 4(c)). On the other hand, although $S^{2-}/S_2^{2-}$ and Sb(III) cannot easily form stable precipitates under high soil pH (Fig. S6(c) and Reaction (13)) (Filella et al., 2002), the binding ability between Sb(III) and $S^{2-}/S_2^{2-}$ (Reactions (14) and (15)) is much higher than that between As(III) and $S^{2-}/S_2^{2-}$ (Table S6). Hence, Sb(III) may be strongly adsorbed by Fe sulfides. Accordingly, the organic bound Sb (including the S associated form) in soil showed an increasing trend during the entire growth period of the rice (Fig. S7).

$$Sb_2O_5 + 6H^+ + 4e^- = 2Sb(OH)_2^+ + H_2O, pe^{0a} = 9.8 \tag{11}$$

$$\equiv Fe_xO_y(OH)_z + Sb(OH)_3 \leftrightarrow Fe_xO_y(OH)_z \cdot Sb(OH)_3 \tag{12}$$

$$Sb^{3+} + 2S^{2-} \rightarrow SbS_2^- \tag{13}$$

$$\equiv FeS_2 + Sb(OH)_3 \leftrightarrow \equiv FeS_2 \cdot Sb(OH)_3 \tag{14}$$

$$\equiv FeS + Sb(OH)_3 \leftrightarrow \equiv FeS \cdot Sb(OH)_3 \tag{15}$$

The RF model was also used for quantitative evaluation of the relative contribution of environmental factors to the Sb content of the total rice plants. The variable importance and partial dependence of the responses of environmental factors including ORP, AVS, Oxalate-Fe, Dis-$Fe^{2+}$/TFe, arrA gene copies, Dis-Sb(III), Dis-TSb, $(NH_4)_2SO_4$-Sb, $NH_4H_2PO_4$-Sb, and Oxalate-Sb to changes in the Sb content in the total rice plants are shown in Fig. 6(c); the pseudo-$R^2$ value in this RF model is 78.53%. The top contributors to the Sb content in the total rice plants were Dis-$Fe^{2+}$, arrA-copies, $NH_4H_2PO_4$-Sb, Oxalate-Fe, AVS, Dis-TSb, Dis-TFe, and $(NH_4)_2SO_4$-Sb with corresponding importance scores of 13.7%, 13.5%, 12.6%, 12.3%, 11.2%, 9.9%, 7.9%, and 7.7%, respectively. These results indicate that the Fe species, Sb(V) reduction, and AVS may determine the Sb content in rice plants. Therefore, the Sb availability was likely controlled by the reductive dissolution of Fe minerals and the reduction of Sb(V) and sulfate.

## 5. Conclusion

Under flooding conditions, the mobility and bioavailability of Cd, As, and Sb in the alkaline cocontaminated paddy soil showed significant differences throughout the growth period of rice plants. It is likely that, with decreases in pH and ORP, Fe-bearing minerals were reduced, and the Fe oxide-bound Cd, As, and Sb were released, initially yielding their high concentrations in pore water. When anaerobes become dominant in the flooded soil, sulfate reduction may be important, resulting in formation of sulfides and sequestration of Cd via adsorption onto carbonates or Fe sulfides or even binding to $S^{2-}$. It is also likely that the reductions of As(V) and Sb(V) were promoted by microbes, but such reductions appeared to increase the mobility of As and lower mobility of Sb due to the contrast physicochemical properties of As(III) and Sb(III). Our data showed that a portion of resulting Sb(III) was likely adsorbed by Fe oxides or Fe sulfides and were thus immobilized further during the microbial reduction. The concentrations of As in the pore water and rice plants continued to increase over the entire growth cycle whereas the Cd and Sb contents in the pore water increased initially, then decreased. Our results indicate that the differences in the properties of various heavy metals and metalloids should be considered during the remediation of cocontaminated soil.

## Appendix A. Supplementary data

Supplementary data to this article can be found online at https://doi.org/10.1016/j.scitotenv.2019.136204.

## References

Al-Sid-Cheikh, M., Pédrot, M., Dia, A., Guenet, H., Vantelon, D., Davranche, M., Gruau, G., Delhaye, T., 2015. Interactions between natural organic matter, sulfur, arsenic and iron oxides in re-oxidation compounds within riparian wetlands: nanoSIMS and X-ray adsorption spectroscopy evidences. Sci. Total Environ. 515-516, 118–128.

Bak, F., Scheff, G., Jansen, K., 1991. A rapid and sensitive ion chromatographic technique for the determination of sulfate and sulfate reduction rates in freshwater lake sediments. FEMS Microbiol. Lett. 85, 23–30.

Breiman, L., 2001a. Random forests. Mach. Learn. 45, 5–32.

Breiman, L., 2001b. Statistical modeling: the two cultures. Stat. Sci. 16, 199–215.

Cai, Y., Li, L., Zhang, H., 2015. Kinetic modeling of pH-dependent antimony (V) sorption and transport in iron oxide-coated sand. Chemosphere 138, 758–764.

Chuan, M.C., Shu, G.Y., Liu, J.C., 1996. Solubility of heavy metals in a contaminated soil: effects of redox potential and pH. Water Air Soil Poll. 90, 543–556.

Couture, R., Van Cappellen, P., 2011. Reassessing the role of sulfur geochemistry on arsenic speciation in reducing environments. J. Hazard. Mater. 189, 647–652.

Davidson, C.M., Duncan, A.L., Littlejohn, D., Ure, A.M., Garden, L.M., 1998. A critical evaluation of the three-stage BCR sequential extraction procedure to assess the potential mobility and toxicity of heavy metals in industrially-contaminated land. Anal. Chim. Acta 363, 45–55.

Dixit, S., Hering, J.G., 2003. Comparison of Arsenic(V) and Arsenic(III) sorption onto iron oxide minerals: implications for arsenic mobility. Environ. Sci. Technol. 37, 4182–4189.

Einen, J., Thorseth, I.H., Øvreås, L., 2008. Enumeration of Archaea and Bacteria in seafloor basalt using real-time quantitative PCR and fluorescence microscopy. FEMS Microbiol. Lett. 282, 182–187.

El Azhari, A., Rhoujjati, A., El Hachimi, M.L., Ambrosi, J., 2017. Pollution and ecological risk assessment of heavy metals in the soil-plant system and the sediment-water column around a former Pb/Zn-mining area in NE Morocco. Ecotox. Environ. Safe. 144, 464–474.

Fang, W., Wei, Y., Liu, J., 2016. Comparative characterization of sewage sludge compost and soil: heavy metal leaching characteristics. J. Hazard. Mater. 310, 1–10.

Favre, F., Tessier, D., Abdelmoula, M., Génin, J.M., Gates, W.P., Boivin, P., 2002. Iron reduction and changes in cation exchange capacity in intermittently waterlogged soil. Eur. J. Soil Sci. 53, 175–183.

Filella, M., Belzile, N., Chen, Y., 2002. Antimony in the environment: a review focused on natural waters: II. Relevant solution chemistry. Earth Sci. Rev. 59, 265–285.

Fortin, D., Beveridge, T.J., 1997. Microbial sulfate reduction within sulfidic mine tailings: formation of diagenetic Fe sulfides. Geomicrobiol. 14, 1–21.

Fu, L., Li, S., Ding, Z., Ding, J., Lu, Y., Zeng, R.J., 2016. Iron reduction in the DAMO/Shewanella oneidensis MR-1 coculture system and the fate of Fe(II). Water Res. 88, 808–815.

Fulda, B., Voegelin, A., Ehlert, K., Kretzschmar, R., 2013. Redox transformation, solid phase speciation and solution dynamics of copper during soil reduction and reoxidation as affected by sulfate availability. Geochim. Cosmochim. Ac. 123, 385–402.

Guo, X., Wu, Z., He, M., 2009. Removal of antimony(V) and antimony(III) from drinking water by coagulation – flocculation – sedimentation (CFS). Water Res. 43, 4327–4335.

Guo, X., Wu, Z., He, M., Meng, X., Jin, X., Qiu, N., Zhang, J., 2014. Adsorption of antimony onto iron oxyhydroxides: adsorption behavior and surface structure. J. Hzard. Mater. 276, 339–345.

Hartley, W., Edwards, R., Lepp, N.W., 2004. Arsenic and heavy metal mobility in iron oxide-amended contaminated soils as evaluated by short- and long-term leaching tests. Environ. Pollut. 131, 495–504.

Hashimoto, Y., Yamaguchi, N., 2013. Chemical speciation of cadmium and sulfur K-edge XANES spectroscopy in flooded paddy soils amended with zerovalent iron. Soil Sci. Soc. Am. J. 77, 1189–1198.

Herath, I., Vithanage, M., Bundschuh, J., 2017. Antimony as a global dilemma: geochemistry, mobility, fate and transport. Environ. Pollut. 223, 545–559.

Hinsinger, P., Plassard, C., Tang, C., Jaillard, B., 2003. Origins of root-mediated pH changes in the rhizosphere and their responses to environmental constraints: a review. Plant Soil 248, 43–59.

Hori, T., Muller, A., Igarashi, Y., Conrad, R., Friedrich, M.W., 2010. Identification of iron reducing microorganisms in anoxic rice paddy soil by $^{13}$C-acetate probing. ISME J. 4, 267–278.

Ilgen, A.G., Trainor, T.P., 2011. Sb(III) and Sb(V) sorption onto Al-rich phases: hydrous Al oxide and the clay minerals kaolinite KGa-1b and oxidized and reduced nontronite NAu-1. Environ. Sci. Technol. 46, 843–851.

Islam, F.S., Gault, A.G., Boothman, C., Polya, D.A., Charnock, J.M., Chatterjee, D., Lloyd, J.R., 2004. Role of metal-reducing bacteria in arsenic release from Bengal delta sediments. Nature 430, 68–71.

Jackson, C.R., Dugas, S.L., 2003. Phylogenetic analysis of bacterial and archaeal arsC gene sequences suggests an ancient, common origin for arsenate reductase. BMC Evol. Biol. 3, 1–10.

Järup, L., 2003. Hazards of heavy metal contamination. Brit. Med. Bull. 68, 167–182.

Ke, Y., Chai, L., Min, X., Tang, C., Chen, J., Wang, Y., Liang, Y., 2014. Sulfidation of heavy-metal-containing neutralization sludge using zinc leaching residue as the sulfur source for metal recovery and stabilization. Miner. Eng. 61, 105–112.

Khaokaew, S., Chaney, R.L., Landrot, G., Ginder-Vogel, M., Sparks, D.L., 2011. Speciation and release kinetics of cadmium in an alkaline paddy soil under various flooding periods and draining conditions. Environ. Sci. Technol. 45, 4249–4255.

Kocar, B.D., Herbel, M.J., Tufano, K.J., Fendorf, S., 2006. Contrasting effects of dissimilatory iron(III) and arsenic(V) reduction on arsenic retention and transport. Environ. Sci. Technol. 40, 6715–6721.

Kong, L., Hu, X., He, M., 2015. Mechanisms of Sb(III) oxidation by pyrite-induced hydroxyl radicals and hydrogen peroxide. Environ. Sci. Technol. 49, 3499–3505.

Kulkarni, H.V., Mladenov, N., McKnight, D.M., Zheng, Y., Kirk, M.F., Nemergut, D.R., 2018. Dissolved fulvic acids from a high arsenic aquifer shuttle electrons to enhance microbial iron reduction. Sci. Total Environ. 615, 1390–1395.

Kulp, T.R., Miller, L.G., Braiotta, F., Webb, S.M., Kocar, B.D., Blum, J.S., Oremland, R.S., 2013. Microbiological reduction of Sb(V) in anoxic freshwater sediments. Environ. Sci. Technol. 48, 218–226.

Lear, G., Song, B., Gault, A.G., Polya, D.A., Lloyd, J.R., 2007. Molecular analysis of arsenate-reducing bacteria within Cambodian sediments following amendment with acetate. Appl. Environ. Microbiol. 73, 1041–1048.

Lee, S., Lee, J., Jeong Choi, Y., Kim, J., 2009. In situ stabilization of cadmium-, lead-, and zinc-contaminated soil using various amendments. Chemosphere 77, 1069–1075.

Li, F., Wang, X., Zhou, S., Liu, C., 2004. Reviews on abiotic transformation of organchlorines on the interface of iron oxides and water in red soil colloids. Eco. Environ. 15, 1343–1351 (in Chinese).

Li, Z.Y., Ma, Z.W., van der Kuijp, T.J., Yuan, Z.W., Huang, L., 2014. A review of soil heavy metal pollution from mines in China: pollution and health risk assessment. Sci. Total Environ. 468–469, 843–853.

Li, X., Yang, H., Zhang, C., Zeng, G., Liu, Y., Xu, W., Wu, Y., Lan, S., 2017. Spatial distribution and transport characteristics of heavy metals around an antimony mine area in central China. Chemosphere 170, 17–24.

Li, J., Zheng, B., He, Y., Zhou, Y., Chen, X., Ruan, S., Yang, Y., Dai, C., Tang, L., 2018. Antimony contamination, consequences and removal techniques: a review. Ecotox. Environ. Safe. 156, 125–134.

Liu, C.P., Luo, C.L., Gao, Y., Li, F.B., Lin, L.W., Wu, C.A., Li, X.D., 2010. Arsenic contamination and potential health risk implications at an abandoned tungsten mine, southern China. Environ. Pollut. 158, 820–826.

Liu, G., Tao, L., Liu, X., Hou, J., Wang, A., Li, R., 2013. Heavy metal speciation and pollution of agricultural soils along Jishui River in non-ferrous metal mine area in Jiangxi Province, China. J. Geochem. Explore. 132, 156–163.

Lovley, D.R., Elizabeth, J.P.P., 1988. Novel mode of microbial energy metabolism: organic carbon oxidation coupled to dissimilatory reduction of iron or manganese. Appl. Environ. Microb. 54, 1472–1480.

Makris, K.C., Sarkar, D., Parsons, J.G., Datta, R., Gardea-Torresdey, J.L., 2009. X-ray absorption spectroscopy as a tool investigating arsenic(III) and arsenic(V) sorption by an aluminum-based drinking-water treatment residual. J. Hzard. Mater. 171, 980–986.

McKeague, J.A., Day, J.H., 1966. Dithionite-and oxalate-extractable Fe and Al as aids in differentiating various classes of soils. Can. J. Soil Sci. 46, 13–22.

Mirza, B.S., Sorensen, D.L., Dupont, R.R., McLean, J.E., 2017. New arsenate reductase gene (arrA) PCR primers for diversity assessment and quantification in environmental samples. Appl. Environ. Microb. 83, 1–27.

Mukhopadhyay, R., Rosen, B.P., Phung, L.T., Silver, S., 2002. Microbial arsenic: from geocycles to genes and enzymes. FEMS Microbiol. Rev. 26, 311–325.

Nadkarni, M.A., Martin, F.E., Jacques, N.A., Hunter, N., 2002. Determination of bacterial load by real-time PCR using a broad-range (universal) probe and primers set. Microbiology 148, 257–266.

Nakamaru, Y.M., Altansuvd, J., 2014. Speciation and bioavailability of selenium and antimony in non-flooded and wetland soils: a review. Chemosphere 111, 366–371.

Ok, Y.S., Usman, A.R.A., Lee, S.S., Abd El-Azeem, S.A.M., Choi, B., Hashimoto, Y., Yang, J.E., 2011. Effects of rapeseed residue on lead and cadmium availability and uptake by rice plants in heavy metal contaminated paddy soil. Chemosphere 85, 677–682.

Okkenhaug, G., Zhu, Y., He, J., Li, X., Luo, L., Mulder, J., 2012. Antimony (Sb) and arsenic (As) in Sb mining impacted paddy soil from Xikuangshan, China: differences in mechanisms controlling soil sequestration and uptake in rice. Environ. Sci. Technol. 46, 3155–3162.

Osborne, T.H., McArthur, J.M., Sikdar, P.K., Santini, J.M., 2015. Isolation of an arsenate-respiring bacterium from a redox front in an arsenic-polluted aquifer in west Bengal, Bengal Basin. Environ. Sci. Technol. 49, 4193–4199.

Pallud, C., Van Cappellen, P., 2006. Kinetics of microbial sulfate reduction in estuarine sediments. Geochim. Cosmochim. Ac. 70, 1148–1162.

Pedersen, H.D., Postma, D., Jakobsen, R., 2006. Release of arsenic associated with the reduction and transformation of iron oxides. Geochim. Cosmochim. Ac. 70, 4116–4129.

Qi, P., Pichler, T., 2016. Sequential and simultaneous adsorption of Sb(III) and Sb(V) on ferrihydrite: implications for oxidation and competition. Chemosphere 145, 55–60.

Qi, P., Pichler, T., 2017. Competitive adsorption of As(III), As(V), Sb(III) and Sb(V) onto ferrihydrite in multi-component systems: implications for mobility and distribution. J. Hazard. Mater. 330, 142–148.

Quéméneur, M., Garrido, F., Billard, P., Breeze, D., Leyval, C., Jauzein, M., Joulian, C., 2016. Bacterial community structure and functional arrA gene diversity associated with arsenic reduction and release in an industrially contaminated soil. Geomicrobiol J. 33, 839–849.

Ren, J.H., Ma, L.Q., Sun, H.J., Cai, F., Luo, J., 2014. Antimony uptake, translocation and speciation in rice plants exposed to antimonite and antimonate. Sci. Total Environ. 475, 83–89.

Reth, S., Reichstein, M., Falge, E., 2005. The effect of soil water content, soil temperature, soil pH-value and the root mass on the soil $CO_2$ efflux - a modified model. Plant Soil 268, 21–33.

Salomon, E., 1998. Extraction of soil potassium with 0.01M calcium chloride compared to official Swedish methods. Commun. Soil Sci. Plant Anal. 29, 2841–2854.

Sheoran, A.S., Sheoran, V., 2006. Heavy metal removal mechanism of acid mine drainage in wetlands: a critical review. Miner. Eng. 19, 105–116.

Sigfusson, B., Meharg, A.A., Gislason, S.R., 2008. Regulation of arsenic mobility on basaltic glass surfaces by speciation and pH. Environ. Sci. Technol. 42, 8816–8821.

Simpson, S.L., 2001. A rapid screening method for acid-volatile sulfide in sediments. Environ. Toxicol. Chem. 20, 2657–2661.

Sun, Y., Polishchuk, E.A., Radoja, U., Cullen, W.R., 2004. Identification and quantification of arsC genes in environmental samples by using real-time PCR. J. Microbiol. Meth. 58, 335–349.

Sun, W., Xiao, E., Dong, Y., Tang, S., Krumins, V., Ning, Z., Sun, M., Zhao, Y., Wu, S., Xiao, T., 2016. Profiling microbial community in a watershed heavily contaminated by an active antimony (Sb) mine in Southwest China. Sci. Total Environ. 550, 297–308.

Sun, W., Xiao, E., Xiao, T., Krumins, V., Wang, Q., Häggblom, M., Dong, Y., Tang, S., Hu, M., Li, B., Xia, B., Liu, W., 2017. Response of soil microbial communities to elevated antimony and arsenic contamination indicates the relationship between the innate microbiota and contaminant fractions. Environ. Sci. Technol. 51, 9165–9175.

Thawornchaisit, U., Polprasert, C., 2009. Evaluation of phosphate fertilizers for the stabilization of cadmium in highly contaminated soils. J. Hazard. Mater. 165, 1109–1113.

Wan, Y., Camara, A.Y., Yu, Y., Wang, Q., Guo, T., Zhu, L., Li, H., 2018. Cadmium dynamics in soil pore water and uptake by rice: influences of soil-applied selenite with different water managements. Environ. Pollut. 240, 523–533.

Wang, Y., Duan, J., Liu, S., Li, W., van Leeuwen, J., Mulcahy, D., 2014. Removal of As(III) and As(V) by ferric salts coagulation – implications of particle size and zeta potential of precipitates. Sep. Purif. Technol. 135, 64–71.

Wang, X., Li, F., Yuan, C., Li, B., Liu, T., Liu, C., Du, Y., Liu, C., 2019. The translocation of antimony in soil-rice system with comparisons to arsenic: alleviation of their accumulation in rice by simultaneous use of Fe(II) and $NO_3^-$. Sci. Total Environ. 650, 633–641.

Weber, F., Hofacker, A.F., Voegelin, A., Kretzschmar, R., 2010. Temperature dependence and coupling of iron and arsenic reduction and release during flooding of a contaminated soil. Environ. Sci. Technol. 44, 116–122.

Wenzel, W.W., Kirchbaumer, N., Prohaska, T., Stingeder, G., Lombi, E., Adriano, D.C., 2001. Arsenic fractionation in soils using an improved sequential extraction procedure. Anal. Chim. Acta 436, 309–323.

Williams, P.N., Lei, M., Sun, G., Huang, Q., Lu, Y., Deacon, C., Meharg, A.A., Zhu, Y., 2009. Occurrence and partitioning of cadmium, arsenic and lead in mine impacted paddy rice: Hunan, China. Environ. Sci. Technol. 43, 637–642.

Wilson, S.C., Lockwood, P.V., Ashley, P.M., Tighe, M., 2010. The chemistry and behaviour of antimony in the soil environment with comparisons to arsenic: a critical review. Environ. Pollut. 158, 1169–1181.

Wilson, S.C., Leech, C.D., Butler, L., Lisle, L., Ashley, P.M., Lockwood, P.V., 2013. Effects of nutrient and lime additions in mine site rehabilitation strategies on the accumulation of antimony and arsenic by native Australian plants. J. Hazard. Mater. 261, 801–807.

Wu, F., Fu, Z., Liu, B., Mo, C., Chen, B., Corns, W., Liao, H., 2011. Health risk associated with dietary co-exposure to high levels of antimony and arsenic in the world's largest antimony mine area. Sci. Total Environ. 409, 3344–3351.

Xiao, E., Krumins, V., Tang, S., Xiao, T., Ning, Z., Lan, X., Sun, W., 2016. Correlating microbial community profiles with geochemical conditions in a watershed heavily contaminated by an antimony tailing pond. Environ. Pollut. 215, 141–153.

Yu, H., Liu, C., Zhu, J., Li, F., Deng, D., Wang, Q., Liu, C., 2016. Cadmium availability in rice paddy fields from a mining area: the effects of soil properties highlighting iron fractions and pH value. Environ. Pollut. 209, 38–45.

Zhang, Y., Chen, Y., Meng, A., Li, Q., Cheng, H., 2008. Experimental and thermodynamic investigation on transfer of cadmium influenced by sulfur and chlorine during municipal solid waste (MSW) incineration. J. Hazard. Mater. 153, 309–319.

Zhao, Z., Jia, Y., Xu, L., Zhao, S., 2011. Adsorption and heterogeneous oxidation of As(III) on ferrihydrite. Water Res. 45, 6496–6504.

Zhao, F., Harris, E., Yan, J., Ma, J., Wu, L., Liu, W., McGrath, S.P., Zhou, J., Zhu, Y., 2013. Arsenic methylation in soils and its relationship with microbial arsM abundance and diversity, and As speciation in rice. Environ. Sci. Technol. 47, 7147–7154.

Zheng, S., Zhang, M., 2011. Effect of moisture regime on the redistribution of heavy metals in paddy soil. J. Environ. Sci.-China 23, 434–443.

Zheng, Y., Bu, N.-S., Long, X.-E., Sun, J., He, C.-Q., Liu, X.-Y., Cui, J., Liu, D.-X., Chen, X.-P., 2017. Sulfate reducer and sulfur oxidizer respond differently to the invasion of Spartina alterniflora in estuarine salt marsh of China. Ecol. Eng. 99, 182–190.

Zhu, Q.H., Huang, D.Y., Ge, T.D., Liu, G.S., Zhu, H.H., Liu, S.L., Zhang, X.N., 2010. Sepiolite is recommended for the remediation of Cd contaminated paddy soil. Acta. Agr. Scand. B-S. P. 60, 110–116.

Zhuang, P., Zou, B., Li, N.Y., Li, Z.A., 2009. Heavy metal contamination in soils and food crops around Dabaoshan mine in Guangdong, China: implication for human health. Environ. Geochem. Hlth. 31, 707–715.